

Notch Activation Induces Endothelial Cell Cycle Arrest and Participates in Contact Inhibition: Role of p21^{Cip1} Repression†

Michela Nosedà,^{1,2} Linda Chang,^{1,3} Graeme McLean,^{1,3} Jonathan E. Grim,⁴
Bruce E. Clurman,⁴ Laura L. Smith,⁴ and Aly Karsan^{1,2,3,5*}

Department of Medical Biophysics¹ and Department of Pathology and Laboratory Medicine,⁵ British Columbia Cancer Agency, and Experimental Medicine Program³ and Department of Pathology and Laboratory Medicine,² University of British Columbia, Vancouver, British Columbia, Canada, and Basic Sciences, Human Biology and Clinical Divisions, Fred Hutchinson Cancer Research Center, Seattle, Washington⁴

Received 11 January 2004/Returned for modification 4 March 2004/Accepted 19 July 2004

Although previous studies demonstrate that appropriate Notch signaling is required during angiogenesis and in vascular homeostasis, the mechanisms by which Notch regulates vascular function remain to be elucidated. Here, we show that activation of the Notch pathway by the ligand Jagged1 reduces the proliferation of endothelial cells. Notch activation inhibits proliferation of endothelial cells in a cell-autonomous manner by inhibiting phosphorylation of the retinoblastoma protein (Rb). During cell cycle entry, p21^{Cip1} is upregulated in endothelial cells. Activated Notch inhibits mitogen-induced upregulation of p21^{Cip1} and delays cyclin D-cdk4-mediated Rb phosphorylation. Notch-dependent repression of p21^{Cip1} prevents nuclear localization of cyclin D and cdk4. The necessity of p21^{Cip1} for nuclear translocation of cyclin D-cdk4 and S-phase entry in endothelial cells was demonstrated by targeted downregulation of p21^{Cip1} by using RNA interference. We further demonstrate that when endothelial cells reach confluence, Notch is activated and p21^{Cip1} is downregulated. Inhibition of the Notch pathway at confluence prevents p21^{Cip1} downregulation and induces Rb phosphorylation. We suggest that Notch activation contributes to contact inhibition of endothelial cells, in part through repression of p21^{Cip1} expression.

The Notch pathway is a highly conserved intercellular signaling mechanism that is activated by interactions of transmembrane ligands of the Jagged (Jagged1 and Jagged2) and Delta (Delta-like 1 [Dll-1], Dll3, and Dll4) families with Notch receptors (Notch1 to -4) expressed on adjacent cells (1). Notch receptors and their ligands have been localized to the vascular endothelium and supporting cells in both the embryo and the adult (12, 20, 27, 34, 35, 37, 41).

Several studies demonstrate that perturbation of the Notch pathway affects vascular development. Mice lacking the Notch ligand Jagged1 die at embryonic day 11.5, exhibiting defects in vascular remodeling. Similar defects are observed in Notch1 null mice (15, 43). Mice that are rendered null for both Notch1 and Notch4 die earlier and show a more severe vascular phenotype than Notch1 null mutants (15). Mice deficient in presenilin-1, which is involved in the cleavage and activation of Notch, show perinatal lethality with a complex phenotype, including abnormal blood vessel development and intracranial hemorrhage (22, 31). Interestingly, vascular defects observed when constitutively active Notch4 is expressed selectively in endothelial cells are also consistent with altered vascular remodeling (17, 40). Hence, mutations inhibiting the Notch path-

way, as well as a sustained activation of Notch, similarly affect vascular development, suggesting that there is a requirement for fine temporal and spatial regulation of Notch signaling. Despite the preponderance of evidence implicating Notch signaling in vascular development, the mechanisms by which Notch exerts its effects on the vasculature remain to be elucidated.

In other systems, Notch signaling determines cell fate by influencing cell proliferation, differentiation, and apoptosis, but the specific effects of Notch activation are related to the cell type and context (1, 38). Activation of the pathway results from engagement of Notch by ligand, which triggers a series of proteolytic cleavages resulting in release of the intracellular portion (NotchIC) from its membrane tether and subsequent nuclear translocation (1). In the nucleus, binding of NotchIC to the transcription factor CBF1 (RBP-J κ) upregulates expression of target genes of the HES (hairy/enhancer of split) and HRT (hairy-related transcription factor) basic helix-loop-helix family of proteins (1, 12).

In the quiescent vasculature of the adult, it is estimated that only 0.01% of cells are actively proliferating (8, 11). In contrast, during angiogenesis, elongation of the new sprout depends on the proliferation of endothelial cells (8, 11). It has been suggested that Notch activation is absent in vessels at the early stages of angiogenesis when endothelial cells are proliferating but that Notch is reactivated when endothelial cells stop proliferating and vessels begin to stabilize (9, 39). Notch activation can stimulate or inhibit proliferation by modulating

* Corresponding author. Mailing address: British Columbia Cancer Research Centre, 601 West 10th Ave., Vancouver, British Columbia, Canada V5Z 1L3. Phone: (604) 877-6248. Fax: (604) 877-6002. E-mail: akarsan@bccrc.ca.

† Supplemental material for this article may be found at <http://mcb.asm.org/>.

cell cycle regulation in a cell type-specific and context-dependent manner (2, 13, 26, 28, 36, 42).

Cell cycle transitions are controlled by cyclin-dependent kinase complexes, which are comprised of regulatory (cyclin) and catalytic (serine-threonine kinase and cdk) subunits (32). Synthesis of D-type cyclins and assembly with their catalytic partners (cdk4 and cdk6) depends upon mitogenic stimulation. Mitogen-dependent nuclear accumulation of cyclin D-dependent kinases initiates the phosphorylation and inhibition of the retinoblastoma gene product (Rb) (32). Rb phosphorylation results in conformational changes that release transcription factors of the E2F family, histone deacetylases, and chromosomal remodeling complexes, thereby promoting expression of target genes necessary for progression towards S phase, including cyclin E and cyclin A (32).

In this report we examine the hypothesis that the Notch pathway is involved in regulation of endothelial cell proliferation. We have previously seen that activated Notch4 does not affect proliferation of simian virus 40 (SV40) large T antigen-transformed endothelial cells (17). Given that SV40 T antigen is able to bind Rb and inhibit its antiproliferative function, we investigated the role of Notch signaling in cell cycle regulation of primary human endothelial cells that express functional Rb. Our results show that Notch activation induces cell cycle arrest in primary endothelial cells via a mechanism that inhibits Rb phosphorylation. Inhibition of Rb phosphorylation is effected by Notch-mediated p21^{Cip1} repression, which reduces cyclin D-cdk4 nuclear targeting and thus Rb phosphorylation activity. Further, endothelial cell-cell contact activates Notch and reduces p21^{Cip1} expression, suggesting that activation of the Notch pathway participates in contact inhibition of endothelial cells.

MATERIALS AND METHODS

Cell culture. The human microvascular endothelial cell line HMEC-1 was provided by the Centers for Disease Control and Prevention (Atlanta, Ga.) (17). Human umbilical vein endothelial cells (HUVEC) were isolated and cultured as previously described (14). Primary human microvascular endothelial cells (HMVEC) and human aortic endothelial cells (HAEC) were purchased from Clonetics and cultured according to manufacturer's instructions. HMEC-1 lines and HUVEC were cultured in MCDB medium (Sigma, St. Louis, Mo.) containing, respectively, 10 or 20% heat-inactivated fetal calf serum (HyClone, Logan, Utah). Cells were incubated for 24 to 48 h in MCDB containing 0.2% serum to synchronize them in G₀. To activate the fusion protein Notch4IC-estrogen receptor (Notch4IC-ER), cells were treated with 250 nM 4-hydroxytamoxifen (4-OHT). In cell synchronization experiments, 4-OHT was added 8 h prior to serum addition. The presenilin inhibitor *N*-[*N*-(3,5-difluorophenacetyl)]-L-alanyl-3-amino-1-methyl-5-phenyl-1,3-dihydro-benzo[*e*](1,4)diazepin-2-one (DFP-AA), was purchased from Calbiochem.

Plasmids and gene transfer. Constructs encoding the C-terminal HA-tagged Notch4IC (17), Notch1IC, and Jagged1 cDNA (a gift of L. Li) were subcloned into the retroviral vector MSCV-IRES-YFP (MIY) (a gift of R. K. Humphries). For the Notch4IC-ER fusion protein, cDNA encoding Notch4IC was subcloned in frame N terminal to the binding domain of the mutated estrogen receptor encoded in the retroviral vector pBabe-hb-ER (a gift of M. McMahon). Endothelial cells were transfected as previously described with the following modifications (17): FuGENE 6 transfection reagent (Roche Diagnostic Corporation, Indianapolis, Ind.) was used for transient transfections of the Amphi Phoenix packaging cell lines, and multiple rounds of infections were performed. pBabe-hb-ER alone was used as a control in experiments based on the inducible system. Expression of Notch4IC, Notch1IC, and Notch4IC-ER fusion protein was confirmed by immunoblotting or immunofluorescence staining after each series of transductions (see Fig. S1 in the supplemental material). cDNA encoding human p21^{Cip1} was obtained from the American Type Culture Collection and subcloned into MIY.

Luciferase assays. The p21-luc construct was obtained by excising the fragment encoding the proximal 2.4-kb region of the human p21 promoter from p53R-green fluorescent protein (a gift from G. Li) (5, 45) and subcloning it into pGL3 Basic vector (Promega Corporation, Madison, Wis.). HA-tagged Notch4IC and Notch1IC were subcloned into pcDNA3 (Invitrogen). For normalization, cells were cotransfected with the *Renilla* Luciferase plasmid pRL-CMV (Promega). Endothelial cells were transfected with SuperFect transfection reagent (Qiagen) according to the manufacturer's recommendations. Dual-luciferase reporter assays (Promega) were performed 48 h after transfection.

RNA interference. Retroviral delivery of interfering short-hairpin RNA (siRNA) constructs was accomplished as previously described (7). Briefly, PCR was used to generate an H1 short-hairpin RNA cassette, which was inserted into the unique *Nhe*I site in the downstream U3 region of the pBabePuro vector. The siRNAs targeting p21^{Cip1} and p27^{Kip1} correspond to nucleotides 431 to 452 (5'-AGACCGCATGACAGATTCTA-3') and 245 to 264 (5'-GCAGCTGCGGAGTTCTAC-3') of each mRNA, respectively.

Reverse transcription-PCR (RT-PCR). Total RNA was isolated by using TRIzol reagent (Invitrogen, Carlsbad, Calif.) and was DNase treated. A control reaction omitting reverse transcriptase was performed in each experiment. PCR was performed with the following primers: Notch1, 5'-CACTGTGGGCGGGTCC-3' and 5'-GTTGTATTGGTTCGGCCACCAT-3'; Notch2, 5'-CCCAATGGGCAAGAAGTCTA-3' and 5'-CACAATGTGGTGGTGGGATA-3'; Notch3, 5'-TGAGACGCTCGTCAGTTCCTT-3' and 5'-TGGAAATGCAGTGAAGTGAGG-3'; Notch4, 5'-TAGGGCTCCCCAGCTCTC-3' and 5'-GGCAGGTGCCCCATT-3'; Jagged1, 5'-CTATGATGAGGGGGATGCt-3' and 5'-CGTCCATTGAGGACTGG-3'; and Dll4, 5'-GCATTGTTTACATTGCATCCTG-3' and 5'-CAAGGGCGTGCGGCTCAAAGTA-3'.

Flow cytometry. For cell cycle analysis, exponentially growing cells were labeled with 5 μ g of Hoechst 33342 (Sigma) per ml for 30 min, trypsinized, and analyzed by flow cytometry as previously described (17). For analysis of bromodeoxyuridine (BrdU) incorporation versus DNA content, cells were labeled with 10 μ M BrdU for 2 h, fixed in 70% ethanol, and treated as previously described (17). Samples were run on an EPICS ELITE-ESP flow cytometer (Beckman Coulter), and data were analyzed by using FCS Express V2 (De Novo Software, Thornhill, Ontario, Canada). Cells were sorted on a FACS 440 instrument (Becton Dickinson).

Immunoblotting. Cells were lysed in radioimmunoprecipitation assay buffer (1% NP-40, 0.5% sodium deoxycholate, 0.1% sodium dodecyl sulfate [SDS]), with addition of fresh protease inhibitor cocktail (Sigma), 0.5 mM phenylmethylsulfonyl fluoride, and phosphatase inhibitors (0.5 mM sodium orthovanadate and 30 mM sodium fluoride). Proteins were quantitated by the D_C protein assay (Bio-Rad Laboratories, Hercules, Calif.). Fifty micrograms of protein was separated by SDS-polyacrylamide gel electrophoresis, and transferred to nitrocellulose membranes (Bio-Rad Laboratories) and developed by enhanced chemiluminescence (PerkinElmer Life Science, Boston, Mass.). The mouse monoclonal antibody against the HA epitope was purchased from BabCo (Richmond, Calif.). Anti-ER, anti-cdk4, anti-cyclin D, anti-p21, anti-p15, anti-p16, and anti-cyclin A antibodies were all obtained from Santa Cruz Biotechnology, Inc (Santa Cruz, Calif.). Anti-p27 antibody was purchased from Transduction Laboratories, anti-Rb (clone G3-245) antibody was purchased from BD Bioscience (Bedford, Mass.), and anti-alpha-tubulin was from Sigma.

cdk4 kinase assay. Cells were treated as described in Results. Lysates from exponentially growing untreated endothelial cells were used as a positive control. Cells were lysed in HEB (50 mM HEPES [pH 7.5], 0.1% Tween, 150 mM NaCl, 1 mM EDTA, 2.5 mM EGTA, 10% glycerol, 1 mM dithiothreitol) containing protease inhibitors and phosphatase inhibitors as described above (with addition of 10 mM glycerolphosphate). Six hundred micrograms of total protein was precleared with protein-G Sepharose beads (Sigma) and incubated with anti-cdk4 antibody (Santa Cruz Biotechnology). Incubation without primary antibody was performed as a negative control. cdk4 complexes were incubated with protein G-Sepharose beads for 30 min. After three washes in HEB and two washes in kinase buffer (20 mM HEPES [pH 7.5], 20 mM MgCl₂, 0.1% β -mercaptoethanol), the beads were suspended in kinase buffer containing Rb-C fusion protein (Rb residues 701 to 928) (Cell Signaling Technology, Beverly, Mass.) and 10 μ Ci of [³²P]ATP per sample (Amersham). Samples were incubated at 30°C for 30 min and separated by SDS-polyacrylamide gel electrophoresis. Phosphorylated Rb was visualized by autoradiography of the dried gels.

Immunofluorescence staining. Cells were fixed in 4% paraformaldehyde, blocked, and permeabilized in phosphate-buffered saline containing 4% fetal calf serum and 0.2% Triton-X. The anti-phospho-Rb antibody (specific for phosphorylation on Ser807/811 on human Rb) was obtained from Cell Signaling Technology. Alexa 594-conjugated or Alexa 488-conjugated secondary antibodies were used according to the recommendations of the manufacturer (Molecular

Probes). For BrdU incorporation, cells were labeled for 2 h with 10 μ M BrdU prior to fixation. The anti-BrdU antibody was conjugated with Alexa 594 (Molecular Probes). Nuclear staining with 4',6'-diamidino-2-phenylindole (DAPI) was used for total cell counts. The proportion of positive cells was determined by counting at least 200 cells per sample. Images were acquired with a 1350EX cooled charge-coupled device digital camera (QImaging, Burnaby, British Columbia, Canada) on a Zeiss Axioplan II Imaging inverted microscope (Carl Zeiss Canada Ltd., Toronto, Ontario, Canada) and analyzed with Northern Eclipse image analysis software (Empix Imaging, Mississauga, Ontario, Canada).

Statistical analysis. To determine statistical significance, a one-way analysis of variance with a Tukey test for multiple comparisons was used in all experiments except for the time course experiments. For the time course experiments, the Mann-Whitney U test was used. Statistical significance was taken at a *P* value of ≤ 0.05 .

RESULTS

Activation of the Notch pathway induces cell cycle arrest in primary endothelial cells. The Notch1 and Notch4 receptors and the Notch ligands Dll4 and Jagged1 have been reported to be expressed in endothelial cells (12). To further define the expression patterns of Notch family members in endothelia of different vascular origins, we analyzed dermal microvascular endothelial cells transformed with SV40 large T antigen (HMEC-1), as well as primary endothelial cells from human dermis-derived microvasculature (HMVEC), human aorta (HAEC), and human umbilical vein (HUVEC). Primary human umbilical artery smooth muscle cells (UASMC) were also tested. Notch1, Notch2, Notch4, and Jagged1 were expressed in all endothelial cells examined (Fig. 1A). Interestingly, Dll4 mRNA was not detected in HMEC-1 and HUVEC, while Notch3 was expressed only in these cells. In agreement with previous reports suggesting that Notch4 is expressed selectively on endothelial cells, UASMC expressed mRNAs of the ligands tested and of all receptors except Notch4 (41).

Given that activation of Notch4 inhibits angiogenesis *in vitro* and *in vivo*, we sought to determine whether Notch4 regulates endothelial cell proliferation. Constitutively active Notch4 (Notch4IC) cDNA was inserted into a retroviral vector (MIY) in which the transgene is linked to yellow fluorescent protein (YFP) through an internal ribosomal entry site (17, 40). HUVEC were transduced with the empty MIY vector (HUVEC-vector) or with vector encoding Notch4IC (HUVEC-Notch4IC). In Fig. 1B we show analysis of the cell cycle distribution in HUVEC-vector and HUVEC-Notch4IC. In HUVEC-Notch4IC, YFP-positive cells (Notch4IC expressing) showed arrest in G_0/G_1 phase, whereas YFP-negative cells (lacking Notch4IC) showed cell cycle profiles similar to those of HUVEC-vector (Fig. 1B and data not shown). Further, in the HUVEC-Notch4IC cultures we observed a reduction of the proportion of YFP-positive cells (Notch4IC expressing) with serial passages, while this was not the case with HUVEC-vector (Fig. 1B [ungated region in the dot plot] and data not shown). This observation provides additional support for a growth-inhibitory effect of Notch4IC. As previously demonstrated, Notch4IC did not affect cell cycle progression in SV40 large-T-antigen-transformed HMEC-1 (data not shown) (17).

Jagged1 is expressed in the endothelial cells tested, and Jagged1 null mice die *in utero* due to vascular defects (43). To determine whether activation of the Notch pathway by the vascular ligand Jagged1 induces cell cycle arrest, we transduced HUVEC with MIY-Jagged1 (HUVEC-Jagged1) or MIY alone (HUVEC-vector). Transduced cells were not se-

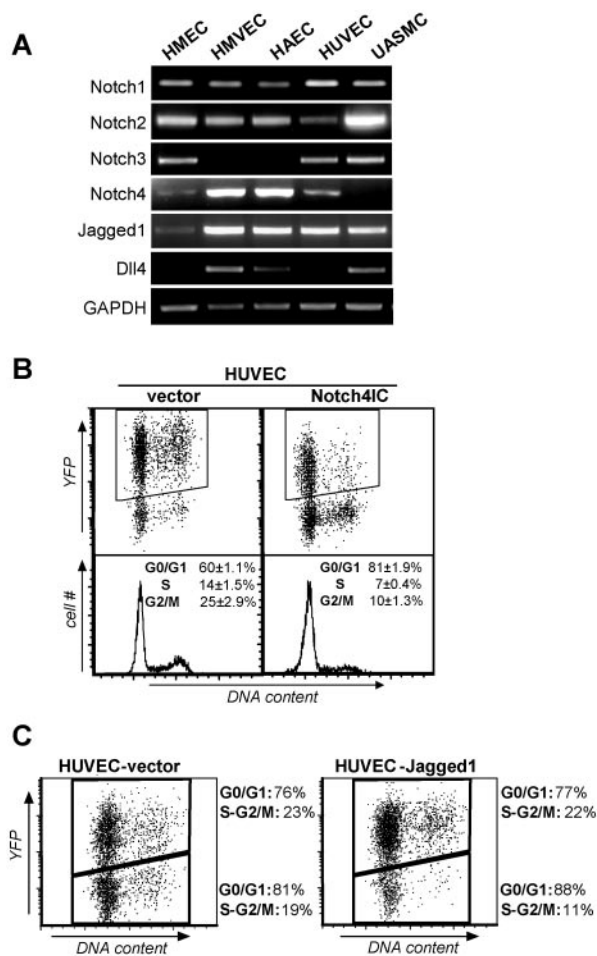


FIG. 1. Notch activation induces cell cycle arrest in primary endothelial cells. (A) RT-PCR for Notch receptors (Notch1, -2, -3, and -4) and ligands (Jagged1 and Dll4). Human endothelial cells from different vascular beds (HMEC, HMVEC, HAEC, and HUVEC) and UASMC were tested. GAPDH, glyceraldehyde-3-phosphate dehydrogenase. (B) Asynchronously growing HUVEC, transduced with MIY (vector) or MIY-Notch4IC (Notch4IC), were labeled with Hoechst 33342 and analyzed by flow cytometry. Dot plots show YFP expression (y axis) and DNA content (x axis). The gated population represents cells expressing YFP. Histograms illustrate cell cycle profiles of HUVEC positive for YFP. Proportions of cells in the G_0/G_1 , S, and G_2/M phases of the cell cycle represent the means from four experiments \pm standard errors of the means. (C) HUVEC transduced with MIY (HUVEC-vector) or MIY-Jagged1 (HUVEC-Jagged1) were labeled with Hoechst 33342 and analyzed by flow cytometry. Dot plots show YFP expression (y axis) and DNA content (x axis). Upper gates represent cells expressing YFP. Lower gates define the YFP-negative population. Cell cycle profiles were analyzed, and the proportions of cells in G_0/G_1 and S- G_2/M are indicated on the right of each gate. Experiments were repeated three times with similar results.

lected for YFP, so Jagged1-expressing cells (YFP positive) existed in coculture with parental HUVEC (YFP negative). We have previously shown that in endothelial cells the overexpression of Jagged1 induces activation of the Notch pathway in a CBF-1-dependent luciferase reporter assay (23). Cell cycle profiles from YFP-positive and YFP-negative populations were compared to study the effect of Jagged1 on cocultured parental HUVEC. In HUVEC-vector cocultures, YFP-nega-

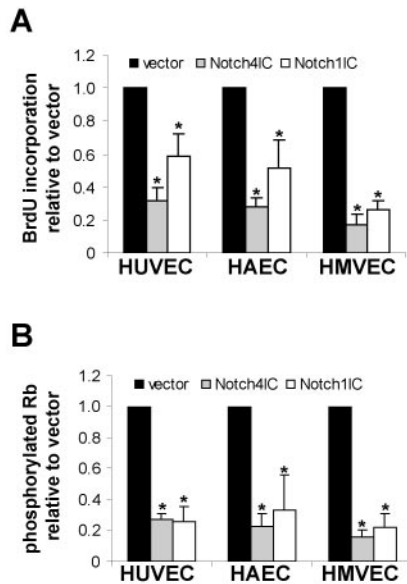


FIG. 2. Notch4IC and Notch1IC inhibit S-phase entry and Rb phosphorylation in endothelial cells from veins, arteries, and microvessels. HUVEC, HAEC, and HMVEC were transduced with MIY (vector), MIY-Notch4IC (Notch4IC), or MIY-Notch1IC (Notch1IC). Asynchronously growing cells were assayed for BrdU incorporation (A) (see also Fig. S2 in the supplemental material) and phosphorylated Rb (B) by immunofluorescence staining and enumerated by fluorescence microscopy. DAPI staining was used to define nuclear localization and for total cell counts. Graphs represent the means \pm standard deviations from at least three experiments. *, $P < 0.05$ compared to vector.

tive and YFP-positive cells showed similar cell cycle profiles (Fig. 1C, left panel). In contrast, in HUVEC-Jagged1 cocultures, HUVEC receiving the Jagged1 signal (YFP-negative) had an increased proportion of cells in G_0/G_1 compared to that in the signaling cells (YFP positive) (Fig. 1C, right panel). Coculture experiments performed with HAEC confirmed similar results (data not shown). These data indicate that Notch inhibits proliferation in endothelial cells in which Notch is activated.

Notch4 and Notch1 inhibit Rb phosphorylation in primary endothelial cells of different vascular origins. Because of the demonstrated synergy of Notch4 and Notch1 *in vivo* during vascular development and the potential redundancy of some of their functions, we investigated whether Notch1 would also inhibit endothelial cell proliferation (15). We transduced HAEC, HMVEC, and HUVEC with MIY alone, MIY-Notch4IC, or MIY-Notch1IC. After sorting for YFP-positive cells, S-phase entry was assayed by BrdU incorporation, using immunofluorescence staining (see Fig. S2 in the supplemental material). In all endothelial cells tested, expression of activated Notch4 or Notch1 reduced the proportion of cells entering S phase (Fig. 2A).

During cell cycle progression, transition through the restriction point is blocked by unphosphorylated or hypophosphorylated Rb (32). Phosphorylation of Rb by cyclin-cdk complexes inactivates Rb and allows the cell to progress towards S phase (32). To determine whether Notch-mediated inhibition of S-phase entry was associated with reduced Rb phosphorylation,

asynchronously growing HAEC, HMVEC, and HUVEC were transduced as described above, stained with an antibody against phosphorylated Rb, and examined by immunofluorescence microscopy. Activated Notch4 and Notch1 reduced the proportion of cells expressing phosphorylated Rb in all types of endothelial cells assayed (Fig. 2B). Hence, both Notch4 and Notch1 negatively regulate S-phase entry by a mechanism that prevents phosphorylation of Rb. This finding is consistent with our data showing the inability of activated Notch to overcome the proliferation advantage conferred by SV40 T antigen, which binds and inhibits Rb (4, 17).

Notch4 and Notch1 downregulate $p21^{Cip1}$ expression and inhibit cyclinD-cdk4 nuclear localization. Studies with murine keratinocytes have shown that Notch1-mediated cell cycle arrest is associated with upregulation of the cyclin-dependent kinase inhibitor (CKI) $p21^{Cip1}$ (26). In small-cell lung cancer cells, Notch-mediated cell cycle arrest is associated with induction of two members of the Cip/Kip CKI family, $p21^{Cip1}$ and $p27^{Kip1}$ (36). To determine whether activated Notch4 or Notch1 also upregulates $p21^{Cip1}$ or $p27^{Kip1}$ in endothelial cells, HUVEC-Notch4IC and HUVEC-Notch1IC were immunoblotted for $p21^{Cip1}$ and $p27^{Kip1}$. Surprisingly, both activated Notch4 and Notch1 inhibited $p21^{Cip1}$ expression in endothelial cells, whereas a statistically significant difference in expression of $p27^{Kip1}$ was not detected (Fig. 3A).

In keratinocytes, induction of $p21^{Cip1}$ expression by Notch depends on a mechanism that induces transcriptional activity of the $p21^{Cip1}$ promoter (26). To determine the effect of constitutively active Notch at the $p21^{Cip1}$ promoter in endothelial cells, we performed promoter-luciferase assays in HUVEC cotransfected with a $p21$ -luc construct and with one of empty vector, Notch4IC or Notch1IC. In contrast to the findings reported for keratinocytes, Notch activation repressed $p21^{Cip1}$ promoter activity in HUVEC (Fig. 3B). These data demonstrate that Notch-mediated $p21^{Cip1}$ downregulation in endothelial cells is also dependent on a transcriptional mechanism, albeit with an opposite effect on the $p21^{Cip1}$ promoter compared to keratinocytes, and they implicate cell-specific nuclear events with respect to the $p21^{Cip1}$ promoter activity in the context of Notch activation.

In addition to acting as inhibitors of cdks, $p21^{Cip1}$ and $p27^{Kip1}$ have been shown to promote activation of cyclin D-dependent kinases, which initiate Rb phosphorylation during cell cycle progression (3, 16). The role of the Cip/Kip proteins as activators of cyclinD-cdk4 complexes depends, at least in part, on their ability to bind and target cyclin D and cdk4 to the nucleus (3, 16). To determine whether the lack of $p21^{Cip1}$ leads to decreased nuclear localization of cyclin D and cdk4 in HUVEC-Notch4IC and HUVEC-Notch1IC, asynchronously growing cells were stained with antibodies against cyclin D and cdk4 (Fig. 4A). Both activated Notch4 and Notch1 dramatically reduced nuclear localization of cdk4 and cyclin D (Fig. 4B). These data suggest that Notch activation may decrease Rb phosphorylation and S-phase entry, in part by preventing nuclear localization of cyclin D-cdk4 through the downregulation of $p21^{Cip1}$.

Nuclear localization of Notch4IC inhibits $p21^{Cip1}$ expression at early phases of cell cycle entry and delays activation of cyclinD-cdk4. Based on the findings described above, we further investigated the role of $p21^{Cip1}$ in Notch-mediated cell

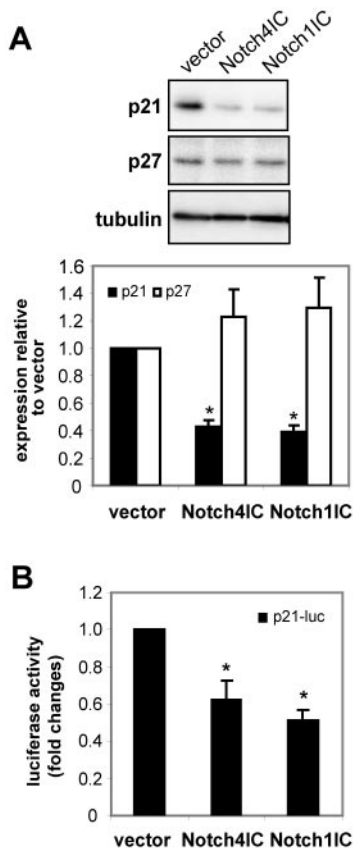


FIG. 3. Activated Notch downregulates p21^{Cip1}. (A) HUVEC transduced with MIY (vector), MIY-Notch4IC (Notch4IC), or MIY-Notch1IC (Notch1IC) were assayed by immunoblotting for p21^{Cip1}, p27^{Kip1}, and tubulin. Immunoblots were analyzed by densitometry and normalized for tubulin. Graphs represent the means ± standard errors of the means from three experiments. *, *P* < 0.001 compared to vector. (B) HUVEC were cotransfected with empty vector (vector), Notch4IC or Notch1IC, a p21 promoter-luciferase construct (p21-luc), and a constitutively active *Renilla* luciferase plasmid. The graphs show relative luciferase activity (means ± standard errors of the means from four experiments, each done in triplicate). *, *P* < 0.01 compared to vector.

cycle arrest. In order to mimic ligand-induced nuclear localization of Notch4IC, we used a tamoxifen (4-OHT)-inducible system based on the fusion of Notch4IC to the mutated ligand-binding domain of the ER (Notch4IC-ER) (29). HUVEC were transduced with the vector encoding Notch4IC-ER (HUVEC-Notch4IC-ER) or with vector alone (HUVEC-vector). Immunostaining demonstrated translocation of the Notch4IC-ER fusion protein to the nucleus following stimulation with 4-OHT (Fig. 5A). Cell counts at 3-day intervals for 9 days demonstrated reduced growth of 4-OHT-treated HUVEC-Notch4IC-ER compared to HUVEC-vector (Fig. 5B). To verify that reduced growth following nuclear translocation of Notch4IC-ER was associated with G₀/G₁ arrest, HUVEC-vector and HUVEC-Notch4IC-ER were assayed for BrdU incorporation and total DNA content in the absence or presence of 4-OHT. Flow cytometry demonstrated reduced S-phase entry in HUVEC-Notch4IC-ER treated with 4-OHT (Fig. 5C). We have recently shown that activation of Notch4 protects

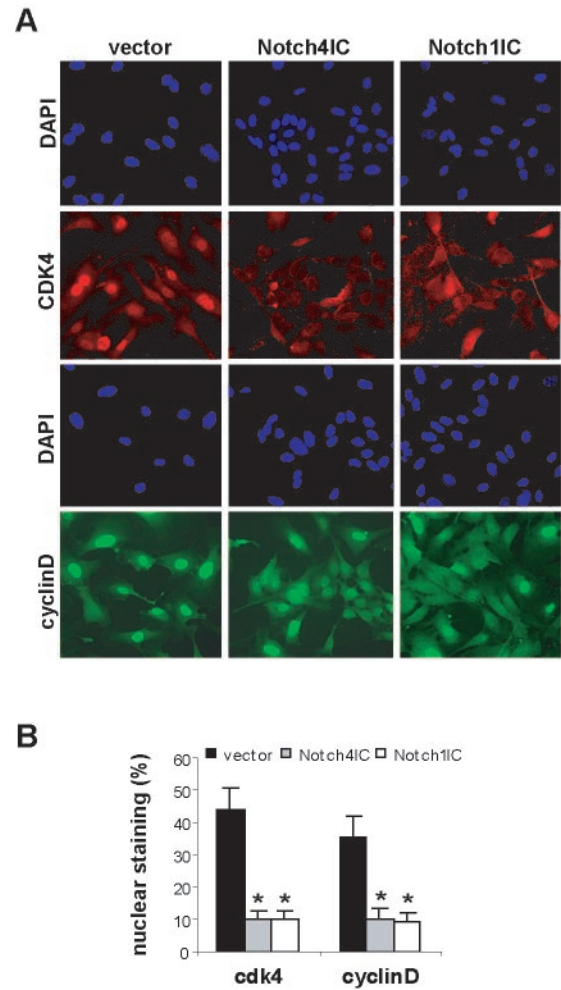


FIG. 4. Activated Notch inhibits nuclear localization of cdk4 and cyclin D. HUVEC transduced with MIY (vector), MIY-Notch4IC (Notch4IC), or MIY-Notch1IC (Notch1IC) were immunostained with antibodies for cdk4 and cyclin D, and the proportion of cells expressing nuclear cdk4 and cyclin D was enumerated by fluorescence microscopy. DAPI staining was used to define nuclear localization and for total cell counts. The graph represents proportions (means ± standard deviations) of cells with prevalent or exclusive nuclear staining from one experiment performed in triplicate. The experiments were repeated twice with similar results. *, *P* < 0.01 compared to vector.

HUVEC against apoptosis, confirming that the inhibition of growth is due to decreased cell proliferation and not to increased apoptosis (19).

To test whether Notch4IC-ER nuclear localization inhibits Rb phosphorylation and to further study the role of Notch4 during cell cycle entry from quiescence, HUVEC were synchronized by serum starvation, pretreated with 4-OHT, and induced to reenter the cell cycle by the addition of serum. Cell cycle profiles were analyzed at the indicated time points, and cell lysates were tested by immunoblotting with an antibody that recognizes both hypophosphorylated and hyperphosphorylated Rb. As expected, upon mitogenic stimulation HUVEC-Notch4IC-ER treated with 4-OHT showed reduced S-phase entry coinciding with a delay in the initiation of Rb phosphorylation (Fig. 5D).

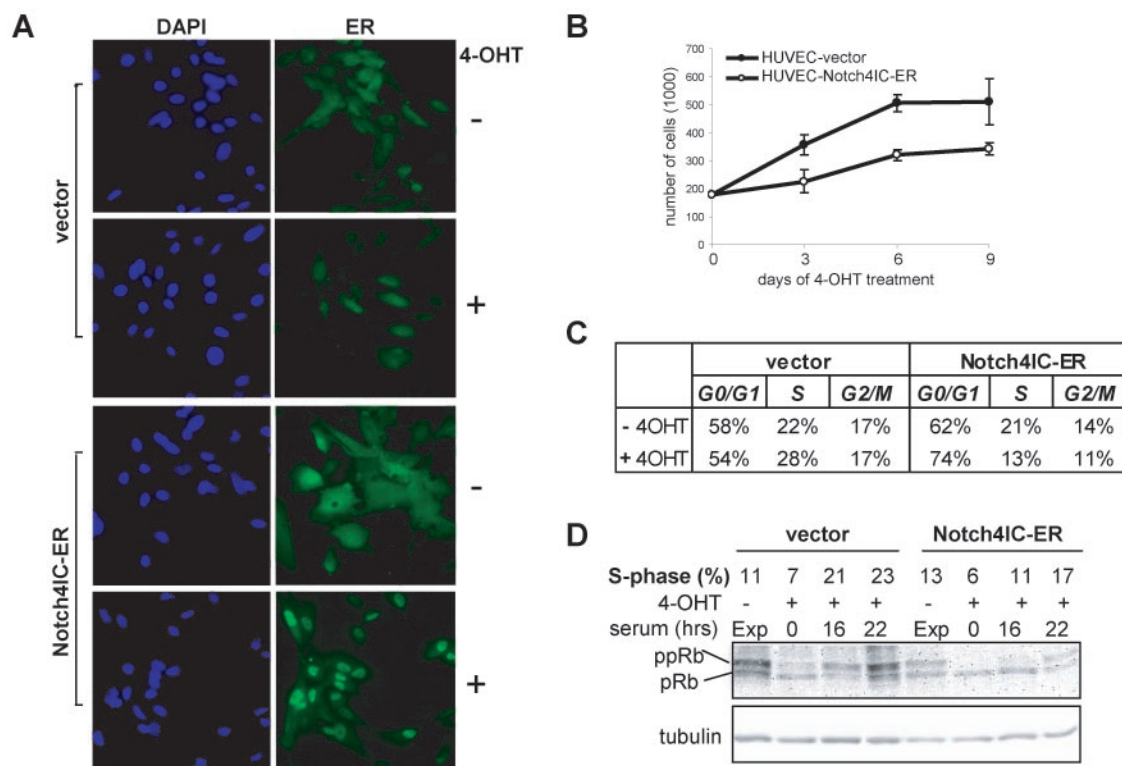


FIG. 5. Translocation to the nucleus of the Notch4IC-ER fusion protein reduces S-phase entry and Rb phosphorylation in HUVEC. HUVEC were transduced with vector alone or vector encoding the Notch4IC-ER fusion protein and selected in puromycin. (A) Cells treated with 4-OHT (+) and treated with vehicle alone (-) were stained with an antibody against ER. DAPI was used for nuclear staining. (B) Cells (2×10^5) were plated (day 0), and medium containing 4-OHT was replaced daily. Cells were counted by trypan blue exclusion after 3, 6, and 9 days. By 6 days, HUVEC-vector reached confluence. The graph shows the means \pm standard deviations for an experiment performed in triplicate. (C) Asynchronously growing HUVEC-vector and HUVEC-Notch4IC-ER were treated for 24 h with 4-OHT (+) or with vehicle alone (-). Cell cycle distributions were analyzed by flow cytometry for BrdU incorporation and DNA content. (D) HUVEC-vector or Notch4IC-ER were synchronized in quiescence by serum starvation and induced to reenter the cell cycle by addition of serum. Cells were treated with 4-OHT (+) to induce Notch4IC-ER nuclear translocation, and asynchronously growing untreated cells (-) were used as a control (Exp). HUVEC were analyzed at the indicated time points by flow cytometry for BrdU incorporation and DNA content and by immunoblotting with an antibody against hypophosphorylated (pRb) and hyperphosphorylated (ppRb) Rb. Tubulin was used as a loading control. The proportion of cells in S phase at each time point is indicated.

Interestingly, in several cell types, $p21^{Cip1}$ is induced following serum stimulation, consistent with a role for $p21^{Cip1}$ as an activator of cyclin D-cdk4 (3, 6, 16, 18, 24, 33). To determine whether serum stimulation upregulates $p21^{Cip1}$ in endothelial cells and whether Notch4 activation inhibits this induction, HUVEC were synchronized by serum starvation and treated as described above. Cells harvested at the indicated time points were tested by immunoblotting for $p21^{Cip1}$ expression. HUVEC-vector showed induction of $p21^{Cip1}$ between 2 and 12 h after serum stimulation, and as expected, this upregulation was inhibited by activation of Notch4IC-ER (Fig. 6A). In contrast, $p27^{Kip1}$ expression was downregulated following serum stimulation, but no differences between HUVEC-vector and HUVEC-Notch4IC-ER were detected (Fig. 6A). To test whether inhibition of $p21^{Cip1}$ induction by Notch4 was associated with reduction of cyclin D-cdk4 kinase activity, cyclin D-cdk4 kinase activity was determined by *in vitro* kinase assay on a C-terminal Rb fusion protein. Delayed and reduced cyclin D-cdk4 kinase activity was observed in HUVEC-Notch4IC-ER following mitogenic stimulation (Fig. 6B). However, there was no difference in cdk4 or cyclin D expression between control

cells and HUVEC-Notch4IC-ER (Fig. 6C; see Fig. S3A in the supplemental material). We also confirmed that $p16^{INK4a}$ (Fig. 6D; see Fig. S3C in the supplemental material) and other CKIs of the INK4 family (data not shown) were not affected by Notch activation. The above data suggest that Notch impairs Rb phosphorylation by preventing induction of $p21^{Cip1}$ and nuclear localization and activation of cyclin D-cdk4 complexes.

$p21^{Cip1}$ is required for nuclear entry of cyclin D-cdk4. Given the inhibitory effect of activated Notch on endothelial cell proliferation and the downregulation of $p21^{Cip1}$ associated with decreased nuclear localization and activation of cyclin D-cdk4, we sought to determine whether reintroduction of $p21^{Cip1}$ into Notch-activated endothelial cells was sufficient to restore nuclear targeting of cyclin D and cdk4. HUVEC-Notch4IC-ER were transduced with MIY vector or MIY encoding $p21^{Cip1}$ (MIY- $p21$). YFP-positive cells were sorted by flow cytometry, and immunofluorescence staining was used to evaluate cyclin D and cdk4 nuclear expression. As expected, control cells (HUVEC-Notch4IC-ER transduced with MIY) treated with 4-OHT to activate Notch4 showed reduced cyclin D and cdk4 nuclear localization compared to vehicle-treated

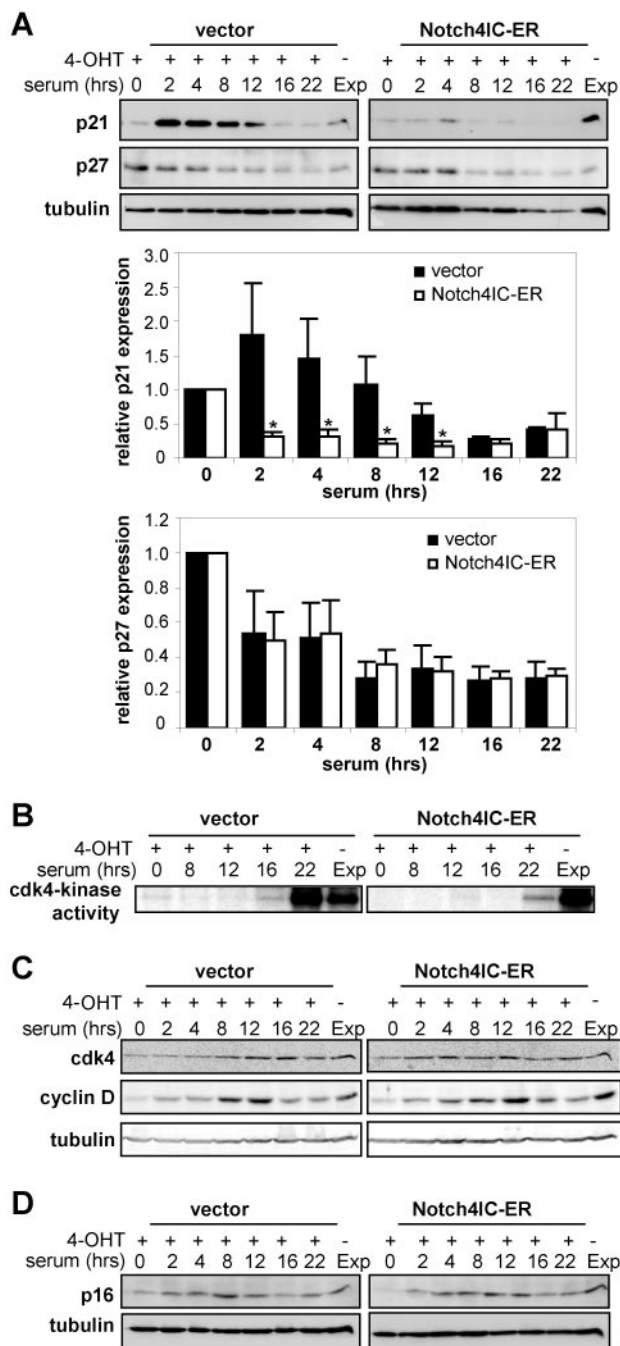


FIG. 6. p21^{Cip1} is required for progression towards S phase in endothelial cells. HUVEC transduced with vector or Notch4IC-ER were synchronized in quiescence by serum starvation and induced to reenter the cell cycle by addition of serum. Cells were treated with 4-OHT (+) to induce Notch4IC-ER nuclear translocation. Untreated (-) asynchronously growing cells were used as a control (Exp). At the indicated times after serum stimulation, cells were assessed for expression of cell cycle regulators. (A) p21^{Cip1} and p27^{Kip1} expression was tested by immunoblotting, analyzed by densitometry, and normalized to tubulin. Graphs represent the means ± standard errors of the means for three experiments. *, P < 0.001. (B) Phosphorylation of a C-terminal Rb fusion protein was tested by in vitro kinase assay of immunoprecipitated cdk4 complexes. (C and D) Expression of cdk4 and cyclin D (C) and p16^{INK4a} (D) was assayed by immunoblotting (see also Fig. S3 in the supplemental material).

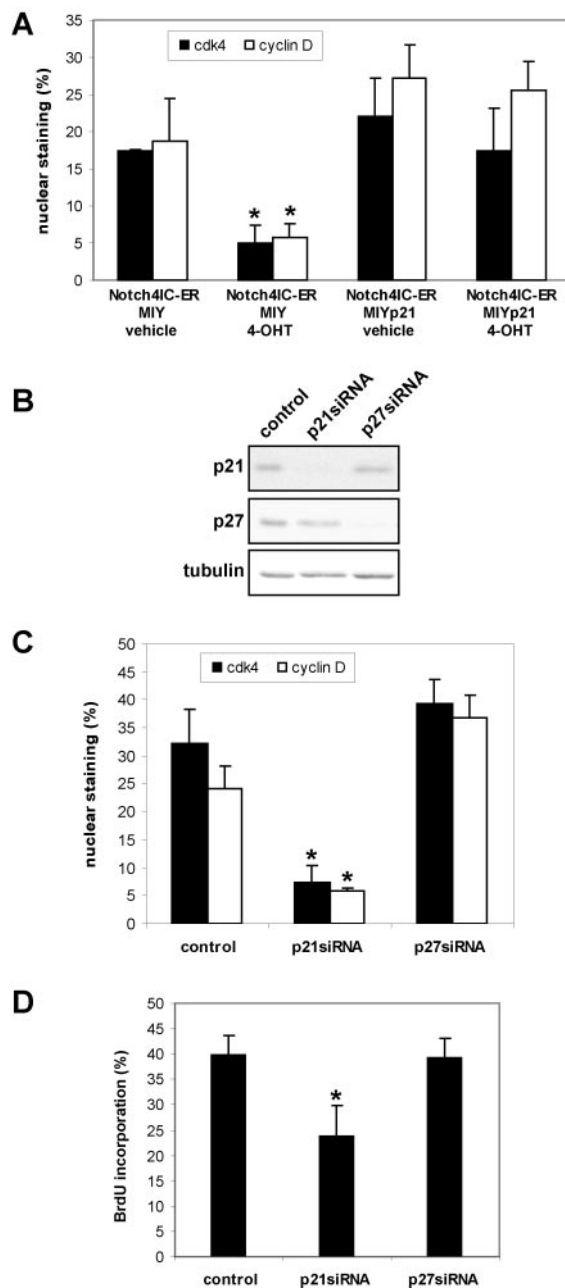


FIG. 7. p21^{Cip1} is essential for cyclin D and cdk4 nuclear localization. (A and B) HUVEC-Notch4IC-ER were transduced with MIY vector (MIY) or MIY encoding p21^{Cip1} (MIYp21). YFP-positive cells were sorted by flow cytometry. Immunofluorescence staining was used to evaluate cyclin D and cdk4 nuclear expression in the presence or absence of 4-OHT. (A) Proportion of cells with prevalent or exclusive cdk4 or cyclin D nuclear staining. The graph represents one experiment done in triplicate (means ± standard deviations) and is representative of two independent experiments. (B, C, and D) Following retroviral delivery of siRNA targeting either p21^{Cip1} (p21siRNA) or p27^{Kip1} (p27siRNA), cells were assayed for expression of p21^{Cip1} and p27^{Kip1} by immunoblotting (B), nuclear localization of cdk4 and cyclin D by immunofluorescence staining (C), and entry into S phase by monitoring BrdU incorporation (D). Empty vector was used as a control. The graph in panel C shows the means ± standard deviations from a single experiment done in triplicate and is representative of two independent experiments. The graph in panel D represents a single experiment done in triplicate (means ± standard deviations) and is representative of three independent experiments. *, P < 0.05.

HUVEC-Notch4IC-ER (Fig. 7A). In contrast, enforced expression of p21^{Cip1} permitted cyclin D and cdk4 nuclear localization despite activation of Notch4 (HUVEC-Notch4IC-ER transduced with MIY-p21 and treated with 4-OHT).

Given the capacity of exogenous p21^{Cip1} to rescue cyclin D-cdk4 nuclear localization, we tested whether downregulation of p21^{Cip1} alone was sufficient to block nuclear localization of cyclin D and cdk4 and to impair cell cycle progression in endothelial cells. Retroviral vectors were used to express siRNA against p21^{Cip1} (p21siRNA) or p27^{Kip1} (p27siRNA) (7). HUVEC were infected with empty vector, p21siRNA, or p27siRNA. After antibiotic selection, exponentially growing cells were tested by immunoblotting for expression of Cip1/Kip1 proteins. In HUVEC, transduction of p21siRNA and p27siRNA specifically decreased expression of p21^{Cip1} and p27^{Kip1}, respectively (Fig. 7B). While cells lacking p21^{Cip1} were defective in targeting cdk4 and cyclin D to the nucleus, the absence of p27^{Kip1} did not affect the nuclear translocation of cdk4 or cyclin D (Fig. 7C). This is not surprising given the fact that only p21^{Cip1} is induced by mitogens in primary endothelial cells entering the cell cycle (Fig. 6A). Furthermore, the lack of p21^{Cip1} was sufficient to reduce S-phase entry in endothelial cells, whereas targeted downregulation of p27^{Kip1} had no effect on this process (Fig. 7D). Taken together, our data provide evidence for a role of p21^{Cip1} in initiating endothelial cell cycle progression, as well as a mechanism for Notch-induced endothelial cell cycle arrest.

Endothelial cell-cell contact activates the Notch pathway and downregulates p21^{Cip1} expression. As we have shown above, endothelial cells from different vascular beds express Notch receptors and their ligands. Cell fate control by Notch during development requires cell-cell contact in a process referred to as lateral inhibition (1). Thus, we hypothesized that endothelial cell-cell contact would activate Notch. To test this hypothesis HUVEC were plated at low density (~30% confluent), medium density (~60% confluent), and high density (100% confluent) and assayed for Notch activation. The Hairy-related transcription factor HRT1 is a target gene of Notch activation in endothelial cells (9, 39). To monitor Notch activation, expression of HRT1 was analyzed by RT-PCR. Up-regulation of HRT1 correlated with increasing confluence of HUVEC (Fig. 8A; see Fig. S4A in the supplemental material) as well as HAEC and HMVEC (data not shown). To determine whether activation of endogenous Notch as a result of cell-cell contact would reduce p21^{Cip1} expression, cell lysates from HUVEC at various levels of confluence were immunoblotted for p21^{Cip1} and p27^{Kip1}. As expected, at high HUVEC density, Notch activation was associated with downregulation of p21^{Cip1} (Fig. 8A; see Fig. S4B in the supplemental material), and as previously described for endothelial and other cell types, HUVEC showed induction of p27^{Kip1} at increasing density (Fig. 8A; see Fig. S4C in the supplemental material) (10, 25). To confirm that the density-dependent downregulation of p21^{Cip1} was mediated by activation of Notch, we used the γ -secretase inhibitor DFP-AA, which inhibits Notch activation by preventing ligand-dependent cleavage of Notch (21, 30, 42). Treatment with DFP-AA abolished downregulation of p21^{Cip1} in HUVEC plated at high density, thus confirming the role of Notch activation (Fig. 8B; see Fig. S4D in the supplemental material). In contrast, induction of p27^{Kip1} was not affected by

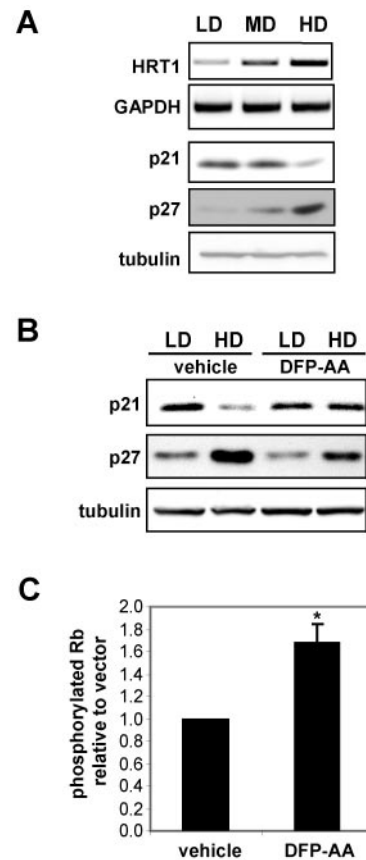


FIG. 8. Endothelial cell-cell interactions activate the Notch pathway and downregulate p21^{Cip1}. (A) HUVEC were plated at low (LD) (~30% confluent), medium (MD) (~60% confluent), and high (HD) (100% confluent) densities. mRNA expression of the Notch target gene HRT-1 and GAPDH was assayed by RT-PCR. Expression of p21^{Cip1} and p27^{Kip1} was assessed by immunoblotting. GAPDH, glyceraldehyde-3-phosphate dehydrogenase. (B) HUVEC at LD and HD were treated with the γ -secretase inhibitor DFP-AA (0.1 μ M) or with vehicle alone, and p21^{Cip1} and p27^{Kip1} expression was assayed by immunoblotting. (C) HUVEC plated at HD underwent 48 h of treatment with DFP-AA (0.1 μ M) or vehicle alone and were stained by immunofluorescence with an antibody against phosphorylated Rb. DAPI staining was used for total cell counts. Graphs represent the means \pm standard errors of the means for four experiments. *, $P < 0.005$. See also Fig. S4 in the supplemental material.

DFP-AA (Fig. 8B; see Fig. S4E in the supplemental material), confirming that regulation of p27^{Kip1} expression does not depend on Notch activation in endothelial cells. To determine whether maintenance of higher levels of p21^{Cip1} as a result of Notch inhibition would promote Rb phosphorylation in confluent endothelial cells, HUVEC at high density were treated with DFP-AA for 2 days and stained by immunofluorescence with an antibody against phosphorylated Rb. The results show an increased proportion of cells expressing phosphorylated Rb in confluent endothelial cells treated with DFP-AA (Fig. 8C), suggesting that inhibition of Notch affects the capacity of confluent endothelial cells to impede cell cycle progression. These findings suggest that Notch activation may be involved in the phenomenon of contact inhibition, in part through downregulation of p21^{Cip1}.

DISCUSSION

The demonstration that Notch activation prevents mitogen-induced p21^{Cip1} upregulation in endothelial cells provides a novel mechanism for Notch-mediated inhibition of proliferation. Our findings suggest that activation of the Notch pathway is involved in the phenomenon of contact inhibition in the endothelium, supporting the hypothesis that Notch participates in the control of vessel homeostasis by maintaining endothelial cell quiescence (9). Interestingly, it has previously been shown that p21^{Cip1} is not expressed in the intima of quiescent adult vessels but is induced 7 days after balloon injury, when a high proportion of cells are proliferating (44). Given the requirement for endothelial cell proliferation during angiogenesis, the antiproliferative effect mediated by Notch explains, at least in part, the defects in vascular remodeling secondary to Notch4 activation in endothelial cells (17, 40). Further, the observation that Notch is not activated early in angiogenesis when endothelial cells begin to proliferate but is reactivated as vessels stabilize complements our data showing that Notch is activated at confluence with concomitant downregulation of p21^{Cip1} (9).

Notch1 is also expressed on endothelial cells, and our data support the notion of a redundancy of function of Notch4 and Notch1 by demonstrating that both members of the Notch family regulate endothelial cell proliferation via a mechanism that converges on inhibition of Rb phosphorylation (15).

Previous studies demonstrate a dual function for p21^{Cip1} that depends on the relative level of expression; low levels of p21^{Cip1} activate cyclin D-*cdk4*, but at higher p21^{Cip1}/cyclin D-*cdk4* stoichiometric ratios, p21^{Cip1} becomes an inhibitor (16, 32). Our studies showing upregulation of p21^{Cip1} upon serum stimulation and downregulation of p21^{Cip1} in confluent endothelial cells imply that p21^{Cip1} has a role in endothelial cell cycle progression. Our data indicate that one mechanism through which Notch interferes with the cell cycle machinery in endothelial cells is the downregulation of p21^{Cip1}, which impairs cyclin D-*cdk4* nuclear localization and activation. We show that exogenous p21^{Cip1} restores cyclin D-*cdk4* nuclear localization in cells expressing activated Notch4. Accordingly, siRNA-targeted downregulation of endogenous p21^{Cip1} hampers nuclear localization of cyclin D and *cdk4* and also impairs the capacity of endothelial cells to enter S phase. Although both p21^{Cip1} and p27^{Kip1} have been reported to shuttle cyclin D and *cdk4* to the nucleus, we show that only targeted knock-down of p21^{Cip1} inhibits cyclin D and *cdk4* nuclear localization in endothelial cells (3, 16). This is likely related to the fact that only p21^{Cip1} is induced during progression towards S phase, whereas p27^{Kip1} is downregulated following serum stimulation but is induced at confluence. Previous studies have shown that murine embryonic fibroblasts that are null for p21^{Cip1} and p27^{Kip1} demonstrate reduced cyclin D-*cdk4* nuclear translocation and Rb kinase activity but no apparent defects in proliferation (3). It is likely that targeted downregulation of p21^{Cip1} by RNA interference in adult cells has an acute effect that cannot be evaded by compensatory mechanisms, as may be seen in gene-targeted animals. Alternatively, p21^{Cip1} may have a role in cell cycle regulation that is cell type specific. The fact that other cell types show upregulation of p21^{Cip1} with Notch activation indicates that Notch-mediated regulation of expres-

sion is modulated by cell-type-specific factors (1, 38). Our data suggest that the specificity of action of Notch on the regulation of p21^{Cip1} expression may depend on cell-type-specific partners of Notch that are involved in the control of the p21^{Cip1} promoter.

Other signaling mechanisms must also be required for Notch-induced cell cycle arrest, since reduction of S-phase entry mediated by targeted downregulation of p21^{Cip1} is not as efficient as the block mediated by Notch. Additionally, Notch must act in concert with other signaling mechanisms, as indicated by a Notch-independent upregulation of p27^{Kip1} at confluence. In conclusion, our studies provide strong evidence that Notch activation participates in the phenomenon of endothelial cell contact inhibition, in part through downregulation of p21^{Cip1}.

ACKNOWLEDGMENTS

We thank F. Wong and I. Pollet for technical help, R. E. Durand and D. McDougal for assistance with flow cytometry and cell sorting, and K. G. Leong for reviewing the manuscript.

This research was supported by grants to A.K. from the Heart and Stroke Foundation of British Columbia and Yukon, the National Cancer Institute of Canada with funds from the Canadian Cancer Society, and the Canadian Institutes of Health Research and to B.E.C. from the NIH (CA84069). M.N. was supported by a fellowship from Fondazione Italiana per la Ricerca sul Cancro, a fellowship from the Canadian Institutes of Health Research, and a Research Trainee Award from the Michael Smith Foundation for Health Research. G.M. was supported by a Research Trainee Award from the Michael Smith Foundation for Health Research. B.E.C. is a W. M. Keck Distinguished Young Scholar in Medical Research. A.K. is a Clinician-Scientist of the Canadian Institutes of Health Research and a Scholar of the Michael Smith Foundation for Health Research.

REFERENCES

1. Artavanis-Tsakonas, S., M. D. Rand, and R. J. Lake. 1999. Notch signaling: cell fate control and signal integration in development. *Science* **284**:770–776.
2. Carlesso, N., J. C. Aster, J. Sklar, and D. T. Scadden. 1999. Notch1-induced delay of human hematopoietic progenitor cell differentiation is associated with altered cell cycle kinetics. *Blood* **93**:838–848.
3. Cheng, M., P. Olivier, J. A. Diehl, M. Fero, M. F. Roussel, J. M. Roberts, and C. J. Sherr. 1999. The p21(Cip1) and p27(Kip1) CDK 'inhibitors' are essential activators of cyclin D-dependent kinases in murine fibroblasts. *EMBO J.* **18**:1571–1583.
4. DeCaprio, J. A., J. W. Ludlow, J. Figge, J. Y. Shew, C. M. Huang, W. H. Lee, E. Marsilio, E. Paucha, and D. M. Livingston. 1988. SV40 large tumor antigen forms a specific complex with the product of the retinoblastoma susceptibility gene. *Cell* **54**:275–283.
5. el-Deiry, W. S., T. Tokino, V. E. Velculescu, D. B. Levy, R. Parsons, J. M. Trent, D. Lin, W. E. Mercer, K. W. Kinzler, and B. Vogelstein. 1993. WAF1, a potential mediator of p53 tumor suppression. *Cell* **75**:817–825.
6. Firpo, E. J., A. Koff, M. J. Solomon, and J. M. Roberts. 1994. Inactivation of a Cdk2 inhibitor during interleukin 2-induced proliferation of human T lymphocytes. *Mol. Cell. Biol.* **14**:4889–4901.
7. Grandori, C., K. J. Wu, P. Fernandez, C. Ngouenet, J. Grim, B. E. Clurman, M. J. Moser, J. Oshima, D. W. Russell, K. Swisshelm, S. Frank, B. Amati, R. Dalla-Favera, and R. J. Monnat, Jr. 2003. Werner syndrome protein limits MYC-induced cellular senescence. *Genes Dev.* **17**:1569–1574.
8. Hanahan, D., and J. Folkman. 1996. Patterns and emerging mechanisms of the angiogenic switch during tumorigenesis. *Cell* **86**:353–364.
9. Henderson, A. M., S. J. Wang, A. C. Taylor, M. Aitkenhead, and C. C. Hughes. 2001. The basic helix-loop-helix transcription factor HESR1 regulates endothelial cell tube formation. *J. Biol. Chem.* **276**:6169–6176.
10. Hirano, M., K. Hirano, J. Nishimura, and H. Kanaide. 2001. Transcriptional up-regulation of p27(Kip1) during contact-induced growth arrest in vascular endothelial cells. *Exp. Cell Res.* **271**:356–367.
11. Hobson, B., and J. Denekamp. 1984. Endothelial proliferation in tumours and normal tissues: continuous labelling studies. *Br. J. Cancer* **49**:405–413.
12. Iso, T., Y. Hamamori, and L. Kedes. 2003. Notch signaling in vascular development. *Arterioscler. Thromb. Vasc. Biol.* **23**:543–553.
13. Jundt, F., I. Anagnostopoulos, R. Forster, S. Mathas, H. Stein, and B. Dorken. 2002. Activated Notch1 signaling promotes tumor cell proliferation and survival in Hodgkin and anaplastic large cell lymphoma. *Blood* **99**:3398–3403.

14. Karsan, A., E. Yee, G. G. Poirier, P. Zhou, R. Craig, and J. M. Harlan. 1997. Fibroblast growth factor-2 inhibits endothelial cell apoptosis by Bcl-2-dependent and independent mechanisms. *Am. J. Pathol.* **151**:1775–1784.
15. Krebs, L. T., Y. Xue, C. R. Norton, J. R. Shutter, M. Maguire, J. P. Sundberg, D. Gallahan, V. Closson, J. Kitajewski, R. Callahan, G. H. Smith, K. L. Stark, and T. Gridley. 2000. Notch signaling is essential for vascular morphogenesis in mice. *Genes Dev.* **14**:1343–1352.
16. LaBaer, J., M. D. Garrett, L. F. Stevenson, J. M. Slingerland, C. Sandhu, H. S. Chou, A. Fattaey, and E. Harlow. 1997. New functional activities for the p21 family of CDK inhibitors. *Genes Dev.* **11**:847–862.
17. Leong, K. G., X. Hu, L. Li, M. Nosedá, B. Larrivee, C. Hull, L. Hood, F. Wong, and A. Karsan. 2002. Activated Notch4 inhibits angiogenesis: role of beta 1-integrin activation. *Mol. Cell. Biol.* **22**:2830–2841.
18. Li, Y., C. W. Jenkins, M. A. Nichols, and Y. Xiong. 1994. Cell cycle expression and p53 regulation of the cyclin-dependent kinase inhibitor p21. *Oncogene* **9**:2261–2268.
19. MacKenzie, F., P. Duriez, F. Wong, M. Nosedá, and A. Karsan. 2004. Notch4 inhibits endothelial apoptosis via RBP-Jkappa-dependent and -independent pathways. *J. Biol. Chem.* **279**:11657–11663.
20. Mailhos, C., U. Modlich, J. Lewis, A. Harris, R. Bicknell, and D. Ish-Horowicz. 2001. Delta4, an endothelial specific notch ligand expressed at sites of physiological and tumor angiogenesis. *Differentiation* **69**:135–144.
21. Micchelli, C. A., W. P. Esler, W. T. Kimberly, C. Jack, O. Berezovska, A. Kornilova, B. T. Hyman, N. Perrimon, and M. S. Wolfe. 2003. Gamma-secretase/presenilin inhibitors for Alzheimer's disease phenocopy Notch mutations in *Drosophila*. *FASEB J.* **17**:79–81.
22. Nakajima, M., S. Yuasa, M. Ueno, N. Takakura, H. Koseki, and T. Shirasawa. 2003. Abnormal blood vessel development in mice lacking presenilin-1. *Mech. Dev.* **120**:657–667.
23. Nosedá, M., G. McLean, K. Niessen, L. Chang, I. Pollet, R. Montpetit, R. Shahidi, K. Dorovini-Zis, L. Li, B. Beckstead, R. E. Durand, P. A. Hoodless, and A. Karsan. 2004. Notch activation results in phenotypic and functional changes consistent with endothelial-to-mesenchymal transformation. *Circ. Res.* **94**:910–917.
24. Nourse, J., E. Firpo, W. M. Flanagan, S. Coats, K. Polyak, M. H. Lee, J. Massague, G. R. Crabtree, and J. M. Roberts. 1994. Interleukin-2-mediated elimination of the p27Kip1 cyclin-dependent kinase inhibitor prevented by rapamycin. *Nature* **372**:570–573.
25. Polyak, K., J. Y. Kato, M. J. Solomon, C. J. Sherr, J. Massague, J. M. Roberts, and A. Koff. 1994. p27Kip1, a cyclin-Cdk inhibitor, links transforming growth factor-beta and contact inhibition to cell cycle arrest. *Genes Dev.* **8**:9–22.
26. Rangarajan, A., C. Talora, R. Okuyama, M. Nicolas, C. Mammucari, H. Oh, J. C. Aster, S. Krishna, D. Metzger, P. Chambon, L. Miele, M. Aguet, F. Radtke, and G. P. Dotto. 2001. Notch signaling is a direct determinant of keratinocyte growth arrest and entry into differentiation. *EMBO J.* **20**:3427–3436.
27. Reaume, A. G., R. A. Conlon, R. Zirngibl, T. P. Yamaguchi, and J. Rossant. 1992. Expression analysis of a Notch homologue in the mouse embryo. *Dev. Biol.* **154**:377–387.
28. Ronchini, C., and A. J. Capobianco. 2001. Induction of cyclin D1 transcription and CDK2 activity by Notch(ic): implication for cell cycle disruption in transformation by Notch(ic). *Mol. Cell. Biol.* **21**:5925–5934.
29. Ronchini, C., and A. J. Capobianco. 2000. Notch(ic)-ER chimeras display hormone-dependent transformation, nuclear accumulation, phosphorylation and CBF1 activation. *Oncogene* **19**:3914–3924.
30. Seiffert, D., J. D. Bradley, C. M. Rominger, D. H. Rominger, F. Yang, J. E. Meredith, Jr., Q. Wang, A. H. Roach, L. A. Thompson, S. M. Spitz, J. N. Higaki, S. R. Prakash, A. P. Combs, R. A. Copeland, S. P. Arneric, P. R. Hartig, D. W. Robertson, B. Cordell, A. M. Stern, R. E. Olson, and R. Zaczek. 2000. Presenilin-1 and -2 are molecular targets for gamma-secretase inhibitors. *J. Biol. Chem.* **275**:34086–34091.
31. Shen, J., R. T. Bronson, D. F. Chen, W. Xia, D. J. Selkoe, and S. Tonegawa. 1997. Skeletal and CNS defects in Presenilin-1-deficient mice. *Cell* **89**:629–639.
32. Sherr, C. J. 2000. Cancer cell cycles revisited. *Cancer Res.* **60**:3689–3695.
33. Sherr, C. J., and J. M. Roberts. 1995. Inhibitors of mammalian G1 cyclin-dependent kinases. *Genes Dev.* **9**:1149–1163.
34. Shirayoshi, Y., Y. Yuasa, T. Suzuki, K. Sugaya, E. Kawase, T. Ikemura, and N. Nakatsuji. 1997. Proto-oncogene of int-3, a mouse Notch homologue, is expressed in endothelial cells during early embryogenesis. *Genes Cells* **2**:213–224.
35. Shutter, J. R., S. Scully, W. Fan, W. G. Richards, J. Kitajewski, G. A. Deblandre, C. R. Kintner, and K. L. Stark. 2000. Dll4, a novel Notch ligand expressed in arterial endothelium. *Genes Dev.* **14**:1313–1318.
36. Sriuranpong, V., M. W. Borges, R. K. Ravi, D. R. Arnold, B. D. Nelkin, S. B. Baylin, and D. W. Ball. 2001. Notch signaling induces cell cycle arrest in small cell lung cancer cells. *Cancer Res.* **61**:3200–3205.
37. Taichman, D. B., K. M. Loomes, S. K. Schachtner, S. Guttentag, C. Vu, P. Williams, R. J. Oakey, and H. S. Baldwin. 2002. Notch1 and Jagged1 expression by the developing pulmonary vasculature. *Dev. Dyn.* **225**:166–175.
38. Talora, C., D. C. Sgroi, C. P. Crum, and G. P. Dotto. 2002. Specific downmodulation of Notch1 signaling in cervical cancer cells is required for sustained HPV-E6/E7 expression and late steps of malignant transformation. *Genes Dev.* **16**:2252–2263.
39. Taylor, K. L., A. M. Henderson, and C. C. Hughes. 2002. Notch activation during endothelial cell network formation in vitro targets the basic HLH transcription factor HESR-1 and downregulates VEGFR-2/KDR expression. *Microvasc. Res.* **64**:372–383.
40. Uyttendaele, H., J. Ho, J. Rossant, and J. Kitajewski. 2001. Vascular patterning defects associated with expression of activated Notch4 in embryonic endothelium. *Proc. Natl. Acad. Sci. USA* **98**:5643–5648.
41. Uyttendaele, H., G. Marazzi, G. Wu, Q. Yan, D. Sassoon, and J. Kitajewski. 1996. Notch4/int-3, a mammary proto-oncogene, is an endothelial cell-specific mammalian Notch gene. *Development* **122**:2251–2259.
42. Weng, A. P., Y. Nam, M. S. Wolfe, W. S. Pear, J. D. Griffin, S. C. Blacklow, and J. C. Aster. 2003. Growth suppression of pre-T acute lymphoblastic leukemia cells by inhibition of notch signaling. *Mol. Cell. Biol.* **23**:655–664.
43. Xue, Y., X. Gao, C. E. Lindsell, C. R. Norton, B. Chang, C. Hicks, M. Gendron-Maguire, E. B. Rand, G. Weinmaster, and T. Gridley. 1999. Embryonic lethality and vascular defects in mice lacking the Notch ligand Jagged1. *Hum. Mol. Genet.* **8**:723–730.
44. Yang, Z. Y., R. D. Simari, N. D. Perkins, H. San, D. Gordon, G. J. Nabel, and E. G. Nabel. 1996. Role of the p21 cyclin-dependent kinase inhibitor in limiting intimal cell proliferation in response to arterial injury. *Proc. Natl. Acad. Sci. USA* **93**:7905–7910.
45. Zhang, W. W., S. Labrecque, E. Azoulay, R. Dudley, and G. Matlashewski. 2001. Development of a p53 responsive GFP reporter; identification of live cells with p53 activity. *J. Biotechnol.* **84**:79–86.